Mon. Not. R. Astron. Soc. **000**, 000–000 (0000) Printed 18 March 2010 (MN LATEX style file v2.2)

The planetary system host HR 8799: On its λ Bootis nature

A. Moya[1⋆], P. J. Amado[2], D. Barrado[1], A. García Hernández[2], M. Aberasturi[1], B. Montesinos[1], F. Aceituno[2]

[1] *Departamento de Astrofísica, Laboratorio de Astrofísica Estelar y Exoplanetas, LAEX-CAB (INTA-CSIC), PO BOX 78, 28691 Villanueva de la Cañada, Madrid, Spain*

[2] *Instituto de Astrofísica de Andalucía - CSIC, Camino Bajo de Huetor 50, 18008, Granada, Spain*

18 March 2010

ABSTRACT

HR 8799 is a λ Bootis, γ Doradus star hosting a planetary system and a debris disk with two rings. This makes this system a very interesting target for asteroseismic studies. This work is devoted to the determination of the internal metallicity of this star, linked with its λ Bootis nature (i.e., solar surface abundances of light elements, and subsolar surface abundances of heavy elements), taking advantage of its γ Doradus pulsations. This is the most accurate way to obtain this information, and this is the first time such a study is performed for a planetary-system-host star. We have used the equilibrium code CESAM and the non-adiabatic pulsational code GraCo. We have applied the Frequency Ratio Method (FRM) and the Time Dependent Convection theory (TDC) to estimate the mode identification, the Brunt-Vaïsälä frequency integral and the mode instability, making the selection of the possible models. When the non-seismological constraints (i.e its position in the HR diagram) are used, the solar abundance models are discarded. This result contradicts one of the main hypothesis for explaining the λ Bootis nature, namely the accretion/diffusion of gas by a star with solar abundance. Therefore, according to these results, a revision of this hypothesis is needed. The inclusion of accurate internal chemical mixing processes seems to be necessary to explain the peculiar abundances observed in the surface of stars with internal subsolar metallicities. The use of the asteroseismological constraints, like those provided by the FRM or the instability analysis, provides a very accurate determination of the physical characteristics of HR 8799. However, a dependence of the results on the inclination angle i still remains. The determination of this angle, more accurate multicolour photometric observations, and high resolution spectroscopy can definitively fix the mass and metallicity of this star.

Key words: stars: abundances – stars: chemically peculiar – stars: fundamental parameters (mass, metallicity) – stars: planetary systems – stars: variables: other – stars: individual: HR8799

1 INTRODUCTION

The A5 V star HR 8799 (V342 Peg, HD 218396, HIP 114189) has been extensively studied in the last years. The first studies of this star were done in the context of asteroseismology. This technique is being developed as an efficient instrument for the study of stellar interiors and evolution (Aerts, Christensen-Dalsgaard, & Kurtz 2010). Through the comparison of the observed pulsational modes with theoretical calculations, the general and internal characteristics of the star can be determined. Schuster & Nissen (1986) firstly reported HR 8799 as a possible SX Phoenicis type. Zerbi et al. (1999) observed this star in a multisite multicolour photometric campaign, with Strömgren filters, and found three independent pulsational frequencies ($f_1 = 1.9791$ c d^{-1} ($\equiv 22.906$ μHz), $f_2 = 1.7268$ c d^{-1} ($\equiv 19.986$ μHz), and $f_3 = 1.6498$ c d^{-1} ($\equiv 19.095$ μHz), units are cycles per day), making it one of the 12 first γ Doradus pulsators known (Kaye et al. 1999). This pulsating stellar group is composed of Main Sequence (MS) stars in the lower part of the classical instability strip (Dupret et al. 2005). Their pulsation modes have periods in the range [0.5,3] days, that is, they are asymptotic g-mode pulsators. Gray & Kaye (1999) obtained an optical spectrum of HR 8799, and assigned an spectral type of kA5 hF0 mA5 V λ Bootis, reporting an atmospheric metallic-

⋆ E-mail: amoya@cab.inta-csic.es

ity of [M/H]=−0.47. They also noted that HR 8799 may be also a Vega-type star, characterized by a far IR excess due to a debris disk. Sadakane (2006) developed a deep study of the metal abundances of this star, confirming its λ Bootis nature (with surface chemical peculiarities).

Two years later, Marois et al. (2008) reported the presence of a planetary system around this star. It was the first detection of such a system carried out by direct imaging. This was the starting point of a set of approximately ten studies about this system during 2009, none of them from the asteroseismic point of view, even considering that the three detected pulsational frequencies can be used to better understand the host star, in particular its λ Bootis nature and evolutionary status.

Discovered by Morgan et al. (1943), the λ Bootis-type stars are non-magnetic, moderately-rotating, Population I stars with spectral types from late B - early A to F (dwarfs)[1], which show peculiarities in the morphology and abundance of the Fe-peak element lines. In particular, these lines are unusually weak considering their spectral types. Significant deficiencies in their abundances (up to 2 dex) are found, whereas C, N, O and S have solar abundance (Paunzen et al. 2002). Different theories have attempted to explain the λ Bootis nature from both observational (photometry, spectroscopy) and theoretical investigations. It is not our aim to discuss all of them here (for a interesting review see Paunzen 2003). Nevertheless, it may be worth describing the most accepted scenario relying on the accretion of inter-stellar medium gas by the star (Venn & Lambert 1990). The accretion/diffusion scenario would explain the abundances found at the base of the outer convective zone of these stars, since convective layers are assumed to remain chemically homogeneous. This accretion/diffusion scenario is based on the accretion of inter-stellar medium by the star, and the mixing of these elements with those of the star due to diffusion and rotationally mixing processes. The accretion rate required to maintain this situation is of the order of 10^{-10}-10^{-14} $M_\odot$ per year (Turcotte & Charbonneau 1993), and, once the accretion has ceased, the metal deficiencies should disappear in approximately 1 Myr due to diffusion and internal mixing processes. Thus, a possible interpretation is that λ Bootis stars are young A-type stars (in a pre-main sequence or zero-age main sequence evolutionary stage), still interacting with their primordial clouds of gas and dust. Interestingly, Paunzen et al. (2002) found that most of the known λ Bootis stars lie between the ZAMS (zero-age main sequence) and the TAMS (terminal-age main sequence, with ages of several hundreds million years). In this case the most likely scenario would be a MS star with solar abundance passing through an interstellar cloud (Kamp & Paunzen 2002). However, the chemical mixing due to internal processes, such as rotationally-induced mixing, cannot be discarded as a possible explanation of the observed abundances.

λ Bootis stars and other types of objects in the same region of the HR diagram, such as δ Scuti and γ Doradus stars, are considered as particularly suitable for the asteroseismological study of poorly known hydrodynamical processes occurring in stellar interiors, like the extent of the convective core, mixing of chemical elements, redistribution of angular momentum (Zahn 1992; Mathis & Zahn 2004; Decressin et al. 2009), etc. λ Bootis-type stars are also pulsating stars. Therefore, asteroseismology can be used to obtain information about the internal structure of these objects. Several works have been devoted to study λ Bootis stars with δ Scuti pulsations, for instance Paunzen (1998); Casas et al. (2009). In addition, the combined use of space and ground-based observations improves the potential of the modelling of the star (Bruntt et al. 2007).

The present work aims at a comprehensive asteroseismic modelling of HR 8799, focusing on the discussion of the λ Bootis nature of the star. More precisely, we want to answer whether the observed abundance is intrinsic to the star or an effect of surface processes. This answer drives the search for possible mechanisms explaining the observed abundances, that is, if there is accretion or not, together with internal chemical transport (rotationally-induced mixing, gravitational settling, radiative levitation, etc.). Up to now, only three λ Bootis stars have been reported to be γ Doradus pulsators: HD 218427 (Rodríguez et al. 2006a), HD 239276 (Rodríguez et al. 2006b), and HR 8799. As γ Doradus stars are asymptotic g-mode pulsators, they are very good candidates for testing the internal structure of the star, in particular its internal metallicity. Some of the most updated tools adapted for this purpose are used: 1) the evolutionary code CESAM (Morel & Lebreton 2008), and 2) the pulsation code GraCo (Moya et al. 2004; Moya and Garrido 2008). Using these tools we performed a massive numerical study of HR 8799 in an attempt of constraining physical and theoretical parameters. In this work we will follow the same scheme used for the study of RV Arietis, 29 Cygnis and 9 Aurigae (Casas et al. 2006, 2009; Moya et al. 2006).

2 OBSERVATIONS AND THE PROPERTIES OF HR 8799

The λ Bootis star HR 8799 was discovered to be a pulsating γ Doradus star by Zerbi et al. (1999). They observed it using multicolour Strömgren photometry and found three frequencies with their corresponding amplitudes and phases in the different wavelenght bands. In Table 1 these frequencies, and the amplitudes and phases for the two highest amplitude frequencies, are shown. Gray & Kaye (1999) obtained spectroscopic observations of this star, providing accurate values for the stellar luminosity, $T_{\rm eff}$, and $\log g$ (see Table 2). They also established the λ Bootis and Vega-type nature of this star. In a study by Sadakane (2006), a more detailed spectroscopic analysis of this star was done. An accurate determination of the individual atmospheric abundances was obtained, confirming the previous results. In a recent paper, Cuypers et al. (2009) carried out a long-term photometric monitoring of a set of γ Doradus stars, including HR 8799. The effective temperature reported in that work is similar to that given in Gray & Kaye (1999).

An interesting additional property of HR 8799 was the observation, by HST and Spitzer, of two well separated rings in its debris disk, located at the inner and the outer limits of the planetary system (Chen et al. 2009; Reidemeister et al. 2009).

[1] Two percent of the A-type stars belong to this class (Gray & Corbally 2002)

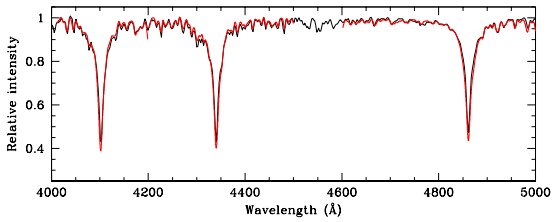

Figure 1. Spectrum of HR 8799 in the interval 4000–5000 Å (black) and, superimposed, a synthetic spectrum computed with $T_{\rm eff}$ = 7430 K, $\log g$ = 4.35, [M/H]=−0.5 and $v \sin i$=37.5 km s^{-1} (red), based on model atmospheres by Kurucz.

2.1 New spectroscopic observations

We have obtained intermediate resolution, high signal-to-noise spectra in the range 3600–7800 Å, with CAFOS (Calar Alto Faint Object Spectrograph) on the 2.2-m telescope at Calar Alto Observatory (CAHA, Almería, Spain). The observations were taken on 9 November 2009. CAFOS was equipped with a CCD SITe detector of 2048×2048 pixels (pixel size 24 μm) and the grisms Blue-100 and Green-100, giving a linear dispersion of ∼ 88 Å/mm (2 Å/pixel).

Spectroscopic observations in the range 3600–6800 Å were also obtained on 12 November 2009 with the spectrograph Albireo on the 1.5-m telescope at the Sierra Nevada Observatory (OSN, Granada, Spain). This instrument is equipped with a CCD2k detector of 2048×2048 pixels. The grating 1200 was used, providing a linear dispersion of ∼ 67 Å/mm (1 Å/pixel).

In both cases the slit width was 1.5 arcsec. The usual bias, dark, dome flat-field and calibration lamp frames were taken. Standard procedures were used to process the data. The widths of the lines of the calibration lamps were used to obtain the instrumental responses of the spectrographs.

2.2 Spectral fitting and properties

The aim of the observations was to carry out a double check of some of the stellar parameters collected from the literature. In Fig. 1 we show the CAFOS spectrum of HR 8799 in the interval 4000–5000 Å (containing the Hβ, Hγ and Hδ Balmer lines) plotted as a black solid line, superimposed by a synthetic spectrum computed using $T_{\rm eff}$ = 7430 K, $\log g$ = 4.35, [M/H]=−0.5 and $v \sin i$=37.5 km s^{-1}. The resolution of the synthetic spectrum has been degraded to match that of the observed one. The agreement between both spectra is quite remarkable, indicating that the stellar parameters used are reliable.

The spectral synthesis has been done using the ATLAS9 and SYNTHE codes by Kurucz (1993). In this work we have used the GNU Linux version of the codes available online[2] (Sbordone et al. 2004). Model atmospheres provided by Castelli & Kurucz (2003) are used as one of the inputs for the synthesis.

Fig. 2 shows the position of HR 8799 in the colour magnitude diagram (CMD). Evolutionary tracks are from Claret (1995). The main sequence has been taken from Philip & Egret (1980) and the δ Scuti instability strip from Rodríguez & Breger (2001). The γ Dor instability strip is from Handler & Shobbrook (2002). Solid stars represent bona fide γ Doradus objects observed by Handler & Shobbrook (2002), and solid triangles are bona fide γ Doradus stars from the literature. The solid and open circles are prime and less probable γ Doradus candidates respectively from those authors. We have derived photometrically $M_{\rm V}$ and $(b-y)_0$ using Strömgren data obtained from the Hauck-Mermilliod catalogue (Hauck & Mermilliod 1998, ;solid star). The reddening correction was negligible. On the other hand, using the Hipparcos parallax (25.38 ± 0.85 mas, i.e., a distance of 39.40 pc), an absolute magnitude M_V=5.96 was calculated. The Hipparcos $M_{\rm V}$ is plotted as an open star. Other available parallaxes in the literature do not change significantly the absolute magnitude of this star (less than 0.1 $L/L_{\odot}$).

The use of different scales of bolometric corrections yields significant larger luminosities (up to 0.3 $L_{\odot}$), compromising the study presented here. We have used the most updated tool provided by Virtual Observatory, VOSA (Bayo et al. 2008) to fit Kurucz atmospheric models to all the photometric observational data available in the literature, avoiding the necessity for estimating the stellar luminosity using bolometric corrections. Models with realistic metallicities, best fitting observations, provide a luminosity similar to that given in Gray & Kaye (1999) (about 0.1 $L/L_{\odot}$ larger).

2.3 Rotation and the limits of our analysis

An important observational uncertainty for the present study comes from the inclination angle i between the rotation axis of the star and the observer line of sight. Using the rotation velocity $v \sin i = 37.5\,{\rm km\,s^{-1}}$ given by Kaye and Strassmeier (1998), several works in the literature tried to provide estimations for i, as in Reidemeister et al. (2009), where one of the detected frequencies have been used as signature of the rotation velocity, obtaining three estimations for the inclination angle, one per observed frequency. The amplitude and phase differences observed in different colour bands for these frequencies make this interpretation invalid. Other determinations of the inclination angle in the literature are related with the observation of the debris disk and/or the dynamics of the planetary system. Fabrycky & Murray-Clay (2010) found a lower limit $i > 20^{\circ}$ based in the dynamical stability of the system, assuming the mass of the planets provided by Marois et al. (2008). On the other hand, Su et al. (2009) studied the debris disk of HR 8799 and found that inclination angles larger than 25° must be ruled out. We have to take this latter result with caution since we must take into account that the morphology inferred from the observations at 70 μm is not a good constraint for the inclination angle of the star. That emission is dominated by a distribution of small grains and the geometry and the inclination angle we derive would correspond to those of disk-like distribution of such particles. That inclination angle may not coincide with the inclination angle of the star (Bate, Lodato, & Pringle 2010).

In the present study, we use the Frequency Ratio Method (FRM) developed in Moya et al. (2005) (see Sec-

[2] `http://wwwuser.oat.ts.astro.it/atmos/`

Table 1. Strömgren multicolour photometric observations. Phase differences and amplitude ratios of filters u, v and b related to filter y for the two frequencies with highest amplitude are also shown.

freq (c/d)	$u-y$ (°)	$v-y$ (°)	$b-y$ (°)	u/y	v/y	b/y
1.9791 (≡ 22.906 μHz)	-0.5±3.6	2.5±2.8	1.8±2.8	0.936±0.057	1.470±0.071	1.275±0.061
1.7268 (≡ 19.986 μHz)	-7.0±7.5	-0.8±5.7	-1.4±5.7	0.830±0.112	1.316±0.137	1.181±0.131
1.6498 (≡ 19.095 μHz)	-	-	-	-	-	-

Table 2. Physical characteristics of HR 8799 taken from: 1) Gray & Kaye (1999) 2) Kaye and Strassmeier (1998) 3) van Leeuwen (2007)

$T_{\rm eff}$ (K)	7430±75	ref. 1
log g (cm s^{-2})	4.35±0.05	ref. 1
$M_{\rm V}$	2.98±0.08	ref. 1
$R(R_\odot)$	1.34±0.05	ref. 1
$L(L_\odot)$	4.92±0.41	ref. 1
$v \sin i$ (km s^{-1})	37.5±2	ref. 2
π (mas)	25.38±0.85	ref. 3

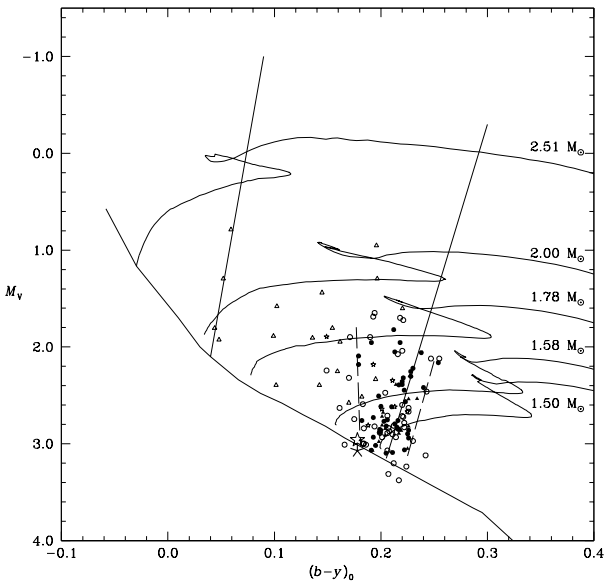

Figure 2. Colour magnitude diagram with absolute visual magnitudes $M_{\rm V}$ plotted against dereddened Strömgren $(b-y)_0$ colour. Small symbols are from Handler & Shobbrook (2002): solid stars represent bona fide γ Doradus stars observed in their work, and solid triangles are bona fide γ Doradus stars from the literature. The small solid and open circles are prime and less probable γ Doradus candidates respectively. The position of HR 8799 is determined by using its Strömgren magnitudes taken from the Hauck-Mermilliod catalogue (Hauck & Mermilliod 1998) and its absolute visual magnitude. Two values were derived for the latter, one derived from the Strömgren photometry using the calibrations by Crawford (1975) and Crawford (1979), implemented in the program TempLogG (Rogers 1995) and another one using the Hipparcos parallax. These two determinations are given in the plot by the larger solid and open star symbols respectively.

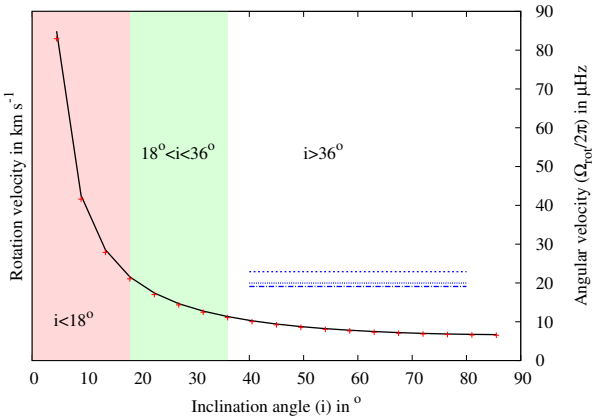

Figure 3. Rotation and angular velocities of HR 8799 as a function of the inclination angle i. The red region ($i < 18°$) represents the zone where the star can hardly be a λ Bootis star. The green region ($18° < i < 36°$) represents the zone where our procedure cannot be applied accurately. The horizontal lines are the observed frequencies of HR 8799.

tion 3.2) for the asteroseismological modelling of this star. This procedure has a limited range of validity in stellar rotation velocity, as demonstrated in Suárez et al. (2005). The rotation velocities used in this work and the pulsational frequencies are around 0.1 and 0.25 of the break-up rotation velocity respectively. Therefore, the use of a second order perturbation theory for the calculation of the frequencies with rotation is accurate enough (Ballot et al. 2009). That second order theory is used for the study done by Suárez et al. (2005). Nevertheless, as the observed frequencies are larger but close to twice the angular rotation velocities used in this work, the use of the traditional approximation to study the accuracy of the asymptotic expression in the presence of rotation would be recommended (Lee & Saio 1987; Townsend 2000; Mathis 2009). This study needs to be carried out to determine more precisely the reliability of the FRM.

In Suárez et al. (2005), the authors found a maximum

rotation velocity of around $60\,\mathrm{km\,s^{-1}}$ for the correct application of the FRM, for a standard γ Doradus star. On the other hand, Turcotte & Charbonneau (1993) found that meridional circulation cannot destroy the accretion pattern (in the accretion/diffusion scenario) for a rotation velocity below $125\,\mathrm{km\,s^{-1}}$. These values provide two lower limits for the inclination angle, one limited by the λ Bootis nature and another one to ensure the applicability of the FRM.

In Figure 3, the rotation velocity as a function of i for a stellar radius of $R = 1.30\,R_\odot$ is shown. For the different stellar radii determined for this star the results are similar. In this figure we see in red the region with $i < 18°$, limit imposed by the λ Bootis nature of HR 8799. In green it is the region with $18° < i < 36°$, the limit for the FRM to be applicable. We want to note that if the inclination angle lies in the green zone, our analysis would be inaccurate. Finally, the observed pulsational frequencies are displayed with horizontal lines. In this figure we see how those frequencies are, at least, twice the rotation frequencies used in this study.

3 TOOLS AND METHODS

In this section, we give a brief description of the tools used for the present study.

3.1 Stellar equilibrium models

The stellar equilibrium models were computed using the evolutionary code CESAM, with a mesh grid (B-splines basis) of 2000 points. First-order effects of rotation on the equilibrium models were considered by subtracting the spherically averaged contribution of the centrifugal acceleration to the gravity of the model, $g_{\rm eff} = g - \mathcal{A}_c(r)$, where g corresponds to the local gravity, and $\mathcal{A}_c(r)$ represents the radial component of the centrifugal acceleration. This spherically averaged component of the centrifugal acceleration does not change the order of the hydrostatic equilibrium equations. Such models are called 'pseudo-rotating' models (see Soufi et al. 1998; Suárez et al. 2007). During evolution, models are assumed to rotate as a rigid body, and their total angular momentum is conserved. Although the non-spherical components of the centrifugal acceleration were not considered, they were included as a perturbation in the computation of the oscillations.

Standard physical inputs for γ Doradus stars are used, i.e., the CEFF equation of state (Christensen-Dalsgaard & Dæppen 1992). The opacity tables were taken from the OPAL package (Iglesias & Rogers 1996), complemented at low temperatures ($T \leqslant 10^4\,\mathrm{K}$) by the tables provided by Alexander & Ferguson (1994). The atmosphere was calculated following two approaches: a grey atmosphere (Eddington $T(\tau)$ law) when the equilibrium models were used to compute adiabatic oscillations, and the Kurucz model atmospheres for the computation of non-adiabatic quantities. The abundance mixture used is that given in Grevesse & Noels (1993).

The main approximation taken in the models with a possible influence in the results of this study is the lack of updated internal chemical transport mechanisms in the equilibrium models, such as rotation-induced mixing or gravitational waves. The inclusion of these mechanisms is the next step to be taken, considering the conclusions obtained in the present work.

3.2 Oscillation computations

The seismic models were completed by computing for each equilibrium model its corresponding oscillation spectrum and non-adiabatic observables.

GraCo (Moya et al. 2004; Moya and Garrido 2008) provides non-adiabatic quantities related to pulsation and includes the convection - pulsation interaction using the Time Dependent Convection theory (Dupret et al. 2005). This theory improves the "frozen convection" approximation usually implemented in most of the codes. With this we can study the instability of the modes. It also provides accurate variations of the effective temperature, effective gravity and phase-lags of the modes. These quantities are the base of the mode identification using multicolour photometry (see Section 3.5). The adiabatic solutions of this code have been used as reference for the ESTA works (Evolution and Asteroseismic Tools Activities, Lebreton et al. 2008; Moya et al. 2008).

3.3 The Frequency Ratio Method

The Frequency Ratio Method or FRM (Moya et al. 2005) takes advantage of the analytical expression of the frequencies given by the asymptotic theory (Tassoul 1980; Smeyers & Moya 2007). γ Doradus stars and other slow pulsators present frequencies in this g-mode asymptotic region. This makes it possible to obtain information of the radial order n of the modes and the Brunt-Väisälä frequency integral of the model, through the ratios of the observed frequencies. With at least three frequencies the method can be carried out.

The application of the method to the three observed frequencies provides chains of $(n_1, \ell_1, n_2, \ell_2, n_3, \ell_3, \mathrm{I_{obs}})$, where n_i is the radial order of mode i, ℓ_i is its spherical order, and $\mathrm{I_{obs}}$ is the new observable introduced by the FRM, the observed Brunt-Väisälä frequency integral, the same for the three frequencies since it is a global property of the stellar model.

Moya et al. (2005) showed that the real solution is part of the set of possible chains provided by the FRM. In addition, in this work we have relaxed the requirement of all the modes having the same ℓ. We allow ℓ to take values 1 or 2, the most probable ones for modes detected with ground-based photometry for γ Doradus stars.

Suárez et al. (2005) showed the application limits of the FRM due to stellar rotation. With the assumption of all the frequencies having the same azimuthal order m, the main conclusions of that paper were: 1) the rotation limit for a standard γ Doradus star for the perturbative approximation to be valid is around $60\,\mathrm{km\,s^{-1}}$, 2) if that assumption is fulfilled, the real solution is still part of the list of possible solutions provided by the FRM, otherwise the FRM does not give any solution, and 3) the accuracy of the asymptotic expressions decreases with the rotation velocity, increasing the number of possible solutions. Nevertheless, these conclusions and application limits of the FRM must be revised under the traditional approximation (see section 2.3).

3.4 Instability analysis

The energy balance of the modes during a complete period is one of the most useful information we can use. Analysing the energy balance of a pulsational mode with its surroundings in a pulsation cycle we can infer if the mode is stable (losses energy) or over-stable (gains energy). To do this study accurately, the main physical processes having influence on this energy balance must be implemented in the codes. Guzik et al. (2000) and Dupret et al. (2005), showed that the position of the base of the the convective envelope is the key point driving γ Doradus modes, since they are originated by the blocking of the radiative flux at this point. This can explain the location of the blue edge of the γ Doradus instability strip. For these stars, the Time Dependent Convection (Dupret et al. 2005; Grigahcène et al. 2005, TDC) is the only set of equations predicting unstable modes in the observed frequency ranges. This development has provided the first theoretical predictions of instability strips for these stars.

3.5 Multicolour photometric analysis

In the following, multicolour photometry is used to provide constraints on the physical characteristics of the star through additional information on the degree ℓ of the spherical harmonic associated to each observed pulsational frequency.

The linear approximation to non-radial flux variations of a pulsating star was first derived by Dziembowski (1977), and later reformulated by Balona & Stobie (1979) and Watson (1988). Then, Garrido et al. (1990) showed that the v and y Strömgren bands can be used for discriminating the degree ℓ. The comparison of the numerical solutions with the observations is based on non-adiabatic calculations (more details in Moya et al. 2004). In particular, pulsation is non-adiabatic in the outer convective zone of these stars, where the thermal relaxation time is of the order of the pulsation period. Accurate determination of the eigenfunctions in these layers, therefore, requires the use of a non-adiabatic description which includes the already mentioned TDC. This procedure makes it possible to relate multicolour photometric observables with such eigenfunctions, allowing therefore a direct constraining on some unknown physical parameters through the direct comparison with observations.

All these tools can be combined to provide an accurate determination of the general physical properties of HR 8799, as described in the next section.

4 ANALYSIS OF THE STAR

The analysis of this star has been done in different steps, imposing the observational constraints sequentially. The sequence is: 1) Fulfill the physical characteristics given by spectroscopy (Gray & Kaye 1999), 2) fulfill the Brunt-Väisälä frequency integral constraints provided by the FRM, 3) predict the observed frequencies to be over-stable, and 4) identify the spherical degree ℓ of the mode for the frequency with the highest amplitude by using the observed multicolour photometry.

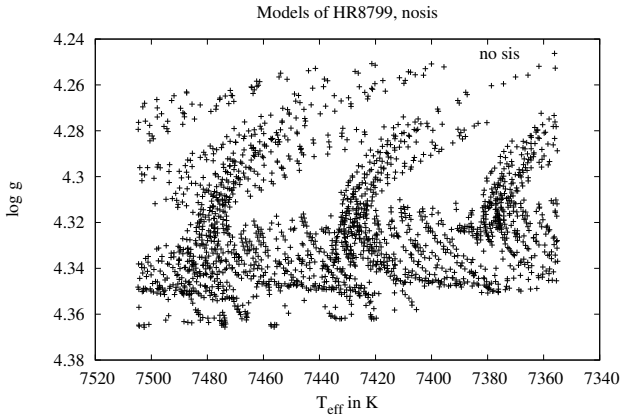

Figure 4. Position on the HR diagram of the models fulfilling the spectroscopic observations. The label "nosis" at the top of the figure means that no seismological constraints are used.

4.1 Position in the HR diagram

The first step of our study was to search for models in a dense grid fulfilling the observed physical characteristics of the star. As it has been explained in Section 2, we have used the effective temperature, luminosity, and gravity (with their errors) given in Table 2. The internal metallicity has been regarded as a free parameter to test the λ Bootis nature of the star and to obtain the internal metallicity using asteroseismology. The mass, estimated in $1.47 \pm 0.30\,M_\odot$ by Gray & Kaye (1999), has been also regarded as a free parameter since it has not been directly determined.

We have developed a grid of CESAM equilibrium models varying the mass (in the range [1.25, 2.10] $M_\odot$ with steps of $0.01 M_\odot$), the metallicity (with values [M/H]=0.08, -0.12, -0.32, and -0.52), the Mixing-Length parameter $\alpha_{\rm MLT}$ (values 0.5, 1, and 1.5), and the overshooting (values 0.1, 0.2, and 0.3).

Figure 4 shows in an HR diagram the models in our grid fulfilling the observations. In Table 3, the range of free parameters of acceptable models is shown. With this first set of observational constraints we have reduced the number of acceptable models from around 600,000 to 1975. This number is still large, but the first main result of this study is that no models with metallicity larger than solar are in the set of acceptable models. To study the reason for this, a new set of models with solar metallicity has been computed. Most of these tracks present models fulfilling all the constraints except the luminosity. In Fig. 5 we present the luminosity as a function of the effective temperature for tracks of different metallicities and masses. All the solar metallicity models present luminosities larger than the observed one for the effective temperatures adopted (represented as a box in the figure).

We conclude, then, that an internal solar metallicity must be discarded for this star. A luminosity $0.2\ L/L_\odot$ larger or a lower effective temperature can make solar metallicity models marginally acceptable. These would be young models located at the ZAMS.

The next goal of this study is to obtain an internal metallicity as accurate as possible with the help of asteroseismology.

Table 3. Acceptable models depending on the physical constraints. Each row shows the results obtained when a new constraint is added with respect to the previous one. The bottom row shows the results obtained when all the constraints are imposed to the less favorable case from the FRM point of view (see text for details). The mass and metallicity determinations are linked, that is, the first mass range is linked with the first metallicity shown, etc.

Constraint	Mass (in $M_\odot$)	Metallicity (in [M/H])	α_{MLT}	Overshooting
HR position	[1.25,1.27],[1.32,1.35],[1.40,1.48]	-0.52, -0.32, -0.12	0.5, 1.0, 1.5	0.1, 0.2, 0.3
Previous + FRM	[1.25,1.27],[1.32,1.34],[1.40,1.48]	-0.52, -0.32, -0.12	0.5, 1.0, 1.5	0.1, 0.2
Previous + Inst	[1.32,1.33],[1.44,1.45]	-0.32, -0.12	1.5	0.1, 0.2
Previous + colours	1.32	-0.32	1.5	0.1, 0.2
Total in less favorable case	[1.32,1.33],[1.44,1.45]	-0.32, -0.12	1.5	0.1, 0.2, 0.3

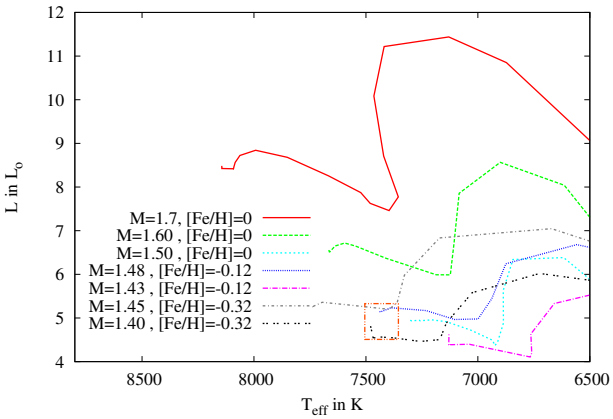

Figure 5. Effective temperature vs. stellar luminosity of some evolutionary tracks (from PMS to ZAMS) with different masses and metallicities, as described in the labels. The box represent the location of valid parameters for HR 8799

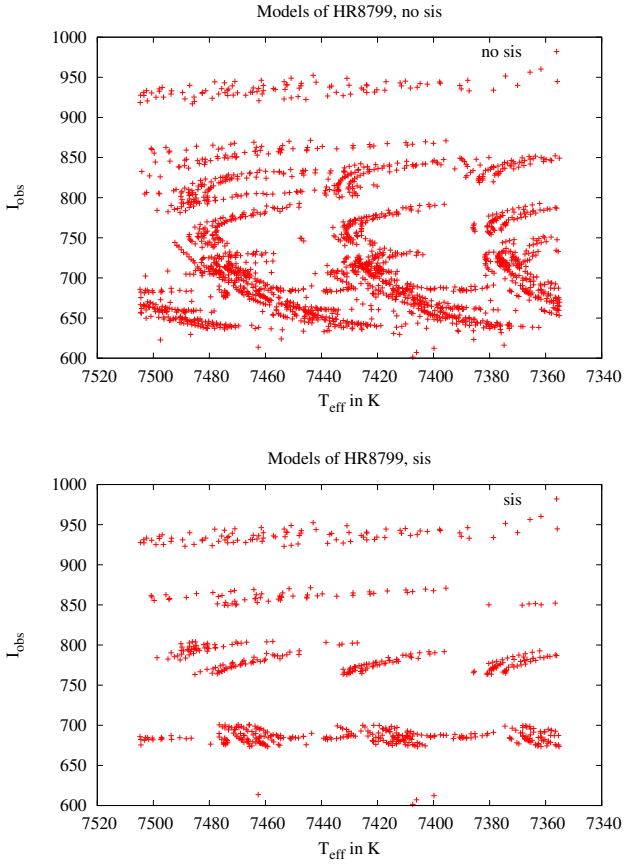

Figure 6. Effective temperature vs. Observed Brunt-Väisälä integral (I_{obs}) obtained with the models fulfilling the spectroscopic constraints (upper panel, no seismological constraints used "no sis") and those restricted by the FRM (bottom panel, seismological constraints "sis").

4.2 Frequency Ratio Method

The observation of three pulsational frequencies in the asymptotic g-mode region makes the FRM suitable for the seismological study of this star. First we must verify if the observed frequencies can be part of the same rotation splitting (making the FRM not valid). This verification is made by taking into account that the largest difference among the observed frequencies is 3.8 μHz. On the other hand, the first order approximation to the rotation splitting provides a difference of the order of the rotation velocity, weighted by a constant usually larger than 0.5 for $\ell = 1$ g-modes and 0.8 for $\ell = 2$ g-modes (Chlebowski 1978). In Figure 3, the smallest rotation velocities, obtained for $i \approx 90^\circ$, are larger than 6.52 μHz. Therefore, the possibility of the two more separate observed frequencies being part of the same splitting is unlikely, since we would need the combination of a Ledoux constant around 0.6 (only possible for some $\ell = 1$ asymptotic g-modes) and, an inclination angle larger than 70°, a very unlikely value for this star taking into account the image obtained of this system, suggesting that the inclination angles are not close to equator-on rotation. This means that the first applicability condition of the FRM is fulfilled.

The second verification of the applicability of the FRM is done on the rotation velocity itself. Suárez et al. (2005) showed that, as the analytical asymptotic expression is developed assuming no rotation, the uncertainty in the application of the expressions grows with the rotation velocity, until a limit where the method cannot be used (as explained in section 3.3).

One of the main assumptions of the FRM is the need that all the frequencies used must have the same azimuthal order m. Currently there is no method that can provide an univocal determination for the value of m, the only one providing some information being optical high-resolution spec-

troscopy. Therefore, we cannot verify this assumption observationally, although there are some indications of the fulfilling of this requirement: 1) The work of Suárez et al. (2005), where the case of modes with different m is studied. Their conclusion is that the procedure is self-consistent. The FRM gives, in that case, no-solutions, but not a wrong solution. This conclusion can be, nevertheless, conditioned by the use of the perturbative approximation. 2) The visibility of the modes with different m in a rotating star is described in Gizon & Solanki (2003). For the inclination angles studied in this work, the visibility of the modes favours those with $m = \pm 1$ in the case of the only mode identified for this star (f_1 having $\ell = 2$, see next sections). Therefore, the only possibility for the observed frequencies to have different m is to have m=1 and $m = -1$. Taking into account the previous study of the value of the rotational splitting, this means that the respective m=0 are well separated and models can only marginally over-stabilize both modes at the same time. In the unlikely case of quasi equator-on inclination angles, the visibility of the modes favours those with $m = \pm 2$, resulting in a larger separation of the corresponding $m = 0$ modes and an even more unlikely over-stabilization of both modes at the same time. The only possible scenario invalidating this assumption is, then, a f_2 having $\ell = 1$ and m=0.

In this work we present two studies for two possible rotation velocities. A first one for a moderate rotation velocity from the point of view of the FRM, around 45 $\mathrm{km\,s^{-1}}$, (this value has been chosen just for illustration purposes because it clearly shows how the procedure used here works). Fabrycky & Murray-Clay (2010) found that this rotation velocity cannot be excluded for HR 8799, acording to the dynamical study of the system. In that case the complete procedure gives very restrictive results regarding the number of accepted models. At the end of the paper (Section 4.5) we show the results obtained for the largest rotation velocity admitted by the FRM (around 60 $\mathrm{km\,s^{-1}}$), where this procedure is less restrictive.

In the case of a rotation velocity of 45 $\mathrm{km\,s^{-1}}$ we have obtained a set of 10 chains, each one with a fixed set of mode identifications and Brunt-Väisälä frequency integral. Fig. 6 shows the set of models fulfilling the additional constraint of $\mathrm{I_{obs}}$ (bottom panel) as compared with those only fulfilling the spectroscopic observations (upper panel). The number of rejected models, for this moderate rotation velocity, is around 70%, but a large number of models is still accepted (see Table 3), and only those with overshooting 0.3 are rejected. This dependence between the Brunt-Väisälä frequency and the overshooting parameter is well known (Miglio et al. 2008) and is part of the valuable information provided by the FRM.

4.3 Instability analysis.

The next step is to verify if the observed modes are predicted to be over-stable for the remaining models, as explained in Section 3.4. Unfortunately, the TDC is not a complete description of the pulsation - convection interaction, and the energy balance provided by this study is not totally accurate. Therefore, we have adopted a conservative criterion for the acceptance of a model: if the modes in the observed frequency range present a growth rate positive or negative but very close to zero, they are accepted. With this criterion, some incorrect models will be considered as acceptable, but we prefer this inconvenience instead of rejecting correct models.

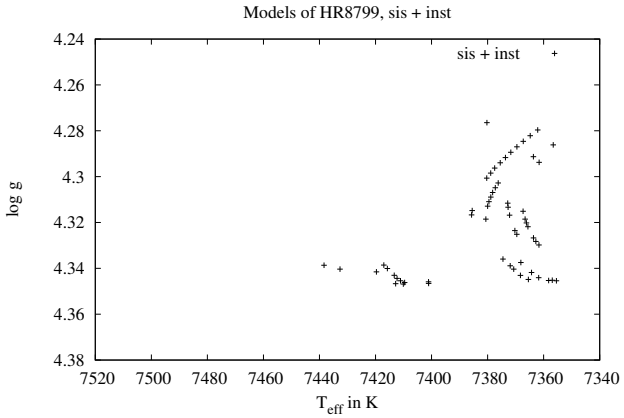

Figure 7. HR diagram position of the models fulfilling the spectroscopic observations + FRM + instability analysis.

This study is robust in selecting models, keeping only 10% of those filtered in the previous step (see Fig. 7 compared with Fig. 4). As the energy balance is a phenomenon mainly thermodynamic, the accepted models are located in a certain $T_{\rm eff}$ range, in the coolest part of the HR diagram. This instability study has also rejected all the models with metallicity -0.52, and $\alpha_{\rm MLT}$ 0.5 and 1.0 (as expected). The remaining valid masses are in the ranges [1.32,1.33] and [1.44,1.45] $\mathrm{M_\odot}$.

4.4 Mode identification with multicolour photometry.

The last step of our study is to use the mode identification from the multicolour photometry obtained for this star (Zerbi et al. 1999). As explained in Section 3.5, the non-adiabatic code, with the TDC implemented, makes it possible to obtain accurate non-adiabatic observables for these stars. With these observables we can carry out the identification of the spherical degree ℓ of the observed modes comparing the theoretical predictions for different modes with observations. In Fig. 8, this comparison, in the phase differences vs. amplitude ratio diagram, is done for a representative model. As all the acceptable models at this stage are in a narrow range of temperatures and masses, the rest of the models provide similar results.

In Fig. 8, the observational errors are displayed as boxes, and only the comparison between bands b and y is made. The comparison of bands v and u with y produce the same type of behaviour. It can be easily checked that the mode f_2 cannot be identified due to its large observational errors, but f_1 is always identified as $\ell = 2$. This is a strong constraint to the models, since the FRM predicts fixed mode identifications for each particular $\mathrm{I_{obs}}$. Therefore, we have to select only those models for which f_1 is predicted to have $\ell = 2$. These models are shown in Fig. 9.

The number of final models fulfilling all the observational constraints is drastically decreased, remaining only 22 models of the initial 1975 models selected not using

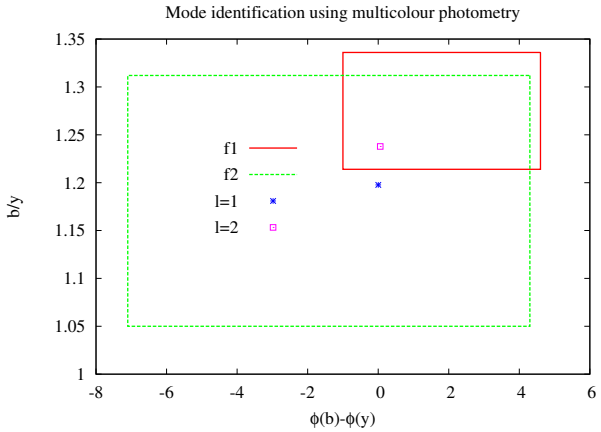

Figure 8. Phase differences vs. amplitude ratio between bands b and y of the two observed frequencies with highest amplitude (boxes) as compared with theoretical predictions for different spherical degrees ℓ (points).

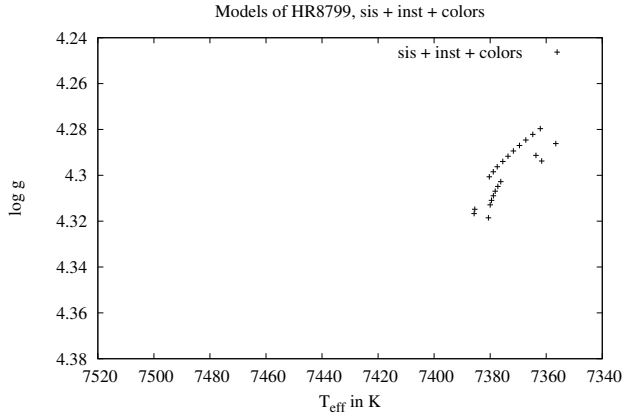

Figure 9. HR diagram position of the models fulfilling the spectroscopic observations + FRM + instability analysis + multicolour photometric mode identification.

asteroseismology. These 22 models have [M/H]=−0.32 ± 0.1 (higher than that given by Gray & Kaye (1999) [M/H]=−0.47 ± 0.1, but consistent with the error bars), M=1.32 ± 0.01 $M_\odot$, α_{MLT} = 1.5 ± 0.3, and overshooting 0.15 ± 0.10.

4.5 The less favourable case

We have already mentioned that the rotation velocity is one of the main uncertainties for this procedure. All the previous studies have been developed assuming a rotation velocity in the middle of the applicability range of the method, that is, with a moderate rotation velocity, or an inclination angle $i = 50°$-$60°$. This may not be the case. Therefore we have also repeated the same procedure for the less favorable case: a rotation velocity around 60 km s^{-1}, which implies an inclination angle around $i \approx 36°$. In this case, the most affected part of the procedure is the FRM, increasing the errors and, as a consequence, the number of acceptable models and I_{obs}. The final result is not as detailed as for the moderate rotating case, and the final set of models fulfilling all the constraints is displayed in Fig. 10. The number of acceptable models is 66, with [M/H]=−0.32 and −0.12, M=[1.32,1.33] and [1.44,1.45] $M_\odot$, α_{MLT} = 1.5, and overshooting= 0.1, 0.2, 0.3. Analysing the differences with the v_{rot} = 45 km s^{-1} case we have noted that the main one is the inclusion of models with overshooting 0.3, making it possible to fulfill the constraints the models with [M/H]=−0.12, and M=[1.44,1.45] $M_\odot$.

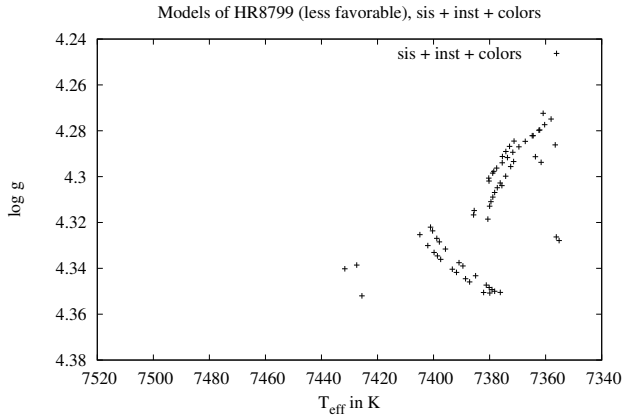

Figure 10. HR diagram position of the models fulfilling the spectroscopic observations + FRM + instability analysis + multicolour photometric mode identification, for the less favourable case in the FRM.

5 CONCLUSIONS AND PERSPECTIVES

In this work, the first comprehensive asteroseismologic study of the planetary system host HR 8799, a λ Bootis star presenting γ Doradus pulsations has been carried out. This asteroseismic work is specially important for the determination of the internal abundances of this kind of stars, a previous step to understand the physical mechanism responsible for the surface chemical peculiarities of the λ Bootis group. The asymptotic g modes observed in HR 8799 make it possible to deeply test its internal metallicity, something hard to do with δ Scuti pulsators, for example.

For the asteroseismologic study, we have used part of the most updated codes and physics for describing γ Doradus stars: CESAM and GraCo codes, TDC theory, FRM, and mode identification using Strömgren multicolour photometry. We have constructed a dense grid of equilibrium models, and carried out a first selection using the available data ($T_{\rm eff}$, log g, and luminosity), leaving the metallicity and mass as free parameters in order to test the internal metallicity of the star.

The first selection shows that there are no models with solar metallicity fulfilling the observations, since the stellar luminosity derived from the observations is smaller than any of the possible luminosities of models with solar metallicity. This contradicts the main assumption of the theories explaining the λ Bootis nature, i.e. that these stars have solar metallicity, whereas the observed abundances are due to surface phenomena.

The asteroseismic study to fix the metallicity of the star

is done using 1) the FRM, to estimate possible mode identifications and Brunt-Väisälä integrals, 2) energy balance to determine the stability of the modes, selecting models in a certain temperature range and $\alpha_{\rm MLT}$ and, 3) mode identification with multicolour photometric observables, selecting only models for which FRM predicts the mode with the highest amplitude to have $\ell = 2$. This is the first time that such a study has been done for a planet-hosting star, but the general procedure was proposed in Moya et al. (2008). All these steps provide a small group of acceptable models depending on the rotation velocity. For a moderate rotation velocity (implying i around 50°) the mass and the metallicity are very precise determined ([M/H]=-0.32 ± 0.1 and M=$1.32 \pm 0.01 M_{\odot}$). For a rotation velocity at the limit of the validity of the FRM (around $i \approx 36°$), the method is less selective and provides some possible values of the metallicity and mass ([M/H]=-0.32 and -0.12 ± 0.1, and M=[1.32,1.33] and [1.44,1.45] $M_{\odot}$ respectively). We point out that inclination angles lower than 18° cannot be possible to preserve the λ Bootis nature of the star. Nevertheless, this limit must be also verified with more accurate observations.

These results have some consequences. The first one is related to the most accepted theory of the λ Bootis nature, namely the accretion/diffusion scenario given by Venn & Lambert (1990). The result of this work, discarding solar metallicity as the internal metallicity of the star, together with the fact that some λ Bootis stars have debris disks not connected with the star (Chen et al. 2009), makes this explanation unlikely, but not negligible (Su et al. 2009). In any case, the equation developed by Venn & Lambert (1990) to describe the individual abundances as a sum of internal abundance plus that of accreted material, must be corrected to include a possible non-solar internal abundance as following

$$\epsilon(m) = (1 - f)\epsilon_*(m) + f\epsilon_{\rm ISM}(m) \quad (1)$$

where f is a mixture factor, and ϵ, ϵ_* and $\epsilon_{\rm ISM}$ are the abundances observed, internal and coming from the interstellar medium of each chemical element, respectively. Therefore, the study of internal chemical mixing processes seems to be the key to explain the λ Bootis nature, at least for HR 8799, as the solar abundances for C, N, O and S observed on its surface have still to be explained.

On the other hand, we have seen that the asteroseismological study needs an accurate determination of the rotation velocity, not just the projected rotation velocity, of the star, for a very accurate determination of the stellar characteristics. Therefore, a consequence of this study is the need for a precise determination of the inclination angle i, of the multicolour photometric amplitudes and phases of f_2, and some information of m values through time-series if high resolution spectroscopy. These determinations would help to carry out a definitive selection of the models.

ACKNOWLEDGMENTS

The authors want to thank an anonymous referee for his/her useful suggestions and comments. AM acknowledges A. Moro-Martín her help and, the financial support from a Juan de la Cierva contract of the Spanish Ministry of Science and Innovation. PJA acknowledges financial support from a "Ramon y Cajal" contract of the Spanish Ministry of Education and Science. This research has been funded by Spanish grants ESP2007-65475-57-C02-02, CSD2006-00070 and ESP2007-65480-C02-01.

REFERENCES

Aerts C., Christensen-Dalsgaard J., Kurtz D. W., 2010, aste.book,
Alexander, D. R. and Ferguson, J. W. 1994, ApJ, 437, 879
Ballot J., Lignières F., Reese D. R., Rieutord M., 2009, arXiv, arXiv:0912.1679
Balona, L. A. and Stobie, R. S. 1979, MNRAS, 189, 649
Bate M. R., Lodato G., Pringle J. E., 2010, MNRAS, 401, 1505
Bayo A., Rodrigo C., Barrado Y Navascués D., Solano E., Gutiérrez R., Morales-Calderón M., Allard F., 2008, A&A, 492, 277
Bruntt H., et al., 2007, A&A, 461, 619
Casas, R. et al. 2006, A&A, 455, 1019
Casas, R. et al. 2009, ApJ, 697, 522
Castelli F., Kurucz R. L., 2003, IAUS, 210, 20P
Chen C. H., Sheehan P., Watson D. M., Manoj P., Najita J. R., 2009, ApJ, 701, 1367
Chlebowski T., 1978, AcA, 28, 441
Christensen-Dalsgaard, J. and Dæppen, W. 1992, A&A Rev., 4, 267
Claret A., 1995, A&AS, 109, 441
Crawford, D. L. 1975, AJ, 80, 955
Crawford D. L., Mandwewala N., 1976, PASP, 88, 917
Crawford, D. L. 1979, AJ, 84, 1858
Cuypers J., et al., 2009, A&A, 499, 967
Decressin, T., Mathis, S., Palacios, A., Siess, L., Talon, S., Charbonnel, C., Zahn, J.-P. 2009, A&A, 495, 271
Dupret, M.-A., Grigahcène, A., Garrido R., et al. 2005, A&A, 435, 927
Dziembowski, W. 1977, Acta Astronomica, 27, 203
Fabrycky D. C., Murray-Clay R. A., 2010, ApJ, 710, 1408
Garrido, R. and Garcia-Lobo, E. and Rodriguez, E. 1990, A&A, 234, 262
Gizon L., Solanki S. K., 2003, ApJ, 589, 1009
Gray, R. O. and Corbally, C. J. 2002, AJ, 124, 989
Gray, R. O. and Kaye, A. B. 1999, AJ, 118, 2993
Grevesse, N., & Noels, A. 1993, Origin and Evolution of the Elements, 14
Grigahcène A., Dupret M.-A., Gabriel M., Garrido R., Scuflaire R., 2005, A&A, 434, 1055
Guzik J. A., Kaye A. B., Bradley P. A., Cox A. N., Neuforge C., 2000, ApJ, 542, L57
Hauck, B. & Mermilliod, M. 1998, A&AS, 129, 431
Handler G., Shobbrook R. R., 2002, MNRAS, 333, 251
Iglesias, C. A. and Rogers, F. J. 1996, ApJ, 464, 943
Kamp, I., & Paunzen, E. 2002, MNRAS, 335, L45
Kaye, A.B. et al. 1999, PASP, 111, 840
Kaye, A.B. and Strassmeier, K.G. 1998, MNRAS, 294, 35
Kurucz R. L., 1993, PhST, 47, 110
Lebreton, Y. et al. 2008, Ap&SS, 316, 1
Lee U., Saio H., 1987, MNRAS, 224, 513
van Leeuwen F., 2007, A&A, 474, 653
Marois, C. et al. 2008, Sci, 322, 1348
Mathis S., 2009, A&A, 506, 811

Mathis, S., Zahn, J.-P. 2004, A&A, 425, 229
Miglio A., Montalbán J., Noels A., Eggenberger P., 2008, MNRAS, 386, 1487
Morel P., Lebreton Y., 2008, Ap&SS, 316, 61
Morgan, W.W. and Keenan, P.C. and Kellman, E. 1943, An atlas of stellar spectra, with an outline of spectrac clasification, (Chicago, I11., The University of Chicago press [1943])
Moya, A. and Garrido, R. and Dupret, M. A. 2004, A&A, 414, 1081
Moya, A. et al. 2005, A&A, 432, 189
Moya, A. et al. 2006, CoAst, 147, 129
Moya, A. and Garrido, R. 2008, Ap&SS, 316, 129
Moya, A. et al. 2008, Ap&SS, 316, 231
Moya A., et al., 2008, AN, 329, 541
Paunzen, E. 1998, Contributions of the Astronomical Observatory Skalnate Pleso, 27, 395
Paunzen, E. and Iliev, I. K. and Kamp, I. and Barzova, I. S. 2002, MNRAS, 336, 1030
Paunzen, E. 2003, Recent. Res. Devel. Astronomy and Astrophysics, 1, 1
Philip A. D., Egret D., 1980, A&AS, 40, 199
Reidemeister M., Krivov A. V., Schmidt T. O. B., Fiedler S., Müller S., Löhne T., Neuhäuser R., 2009, A&A, 503, 247
Rodríguez E., Breger M., 2001, A&A, 366, 178
Rodríguez, E. et al. 2006, A&A, 450, 715
Rodríguez, E. et al. 2006, A&A, 456, 261
Rogers, N. Y. 1995, Communication in Asteroseismology, 78, 1
Sadakane, K. 2006, PASJ, 58, 1023
Sbordone L., Bonifacio P., Castelli F., Kurucz R. L., 2004, MSAIS, 5, 93
Smeyers P., Moya A., 2007, A&A, 465, 509
Schuster, W.J. and Niessen, P.E. 1986, IBVS, 2943
Soufi, F. and Goupil, M. J. and Dziembowski, W. A. 1998, A&A, 334, 911
Su K. Y. L., et al., 2009, ApJ, 705, 314
Suárez, J. C. et al. 2005, A&A, 443, 271
Suárez, J. C. and Garrido, R. and Moya, A. 2007, A&A, 474, 961
Tassoul M., 1980, ApJS, 43, 469
Townsend R. H. D., 2000, MNRAS, 318, 1
Turcotte, S. and Charbonneau, P. 1993, ApJ, 413, 376
Venn, K. A. and Lambert, D. L. 1990, ApJ, 363, 234
Watson, R. D. 1988, AP&SS, 140, 255
Zahn, J.-P. 1992, A&A, 265, 115
Zerbi, F.M., et al. 1999, MNRAS, 303, 275